Çukurova Üniversitesi Mühendislik Mimarlık Fakültesi Dergisi, 34(2), ss. 231-239, Haziran 2019
Çukurova University Journal of the Faculty of Engineering and Architecture, 34(2), pp. 231-239, June 2019

Universal Design Equations for Fractional Order PID Control of Plants with Time Delay

Mehmet Emir KOKSAL[*1]

[1]*Ondokuz Mayıs Üniversitesi, Matematik Bölümü, Samsun*

Geliş tarihi: 01.04.2019 *Kabul tarihi: 28.06.2019*

Universal Design Equations for Fractional Order PID Control of Plants with Time Delay

Abstract

Some all-purpose design equations are derived for designing fractional order controllers for integer order plants with time delay. The results combine many design techniques appearing in the literature. In addition to plotting the global stability boundaries, they can be used to achieve desired gain and phase margins with a flat phase response near the gain cross over frequency. So, robustness can also be guaranteed. Further, satisfactory output disturbance and high frequency noise rejections can be realizable. An example is treated to make connections with the already existing results in the literature, which proves the usability of the obtained design equations.

Keywords: Control design, PID control, Stability

Gerçek Zaman Gecikmeli Rasyonel Transfer Fonksiyonuna Sahip Sistemlerin Kontrolü için Kesirli Mertebeden Oransal-Entegral-Türevsel (PID) Bir Kontrol Edicinin Genel Tasarım Denklemleri

Öz

Herhangi bir gerçek zaman gecikmeli rasyonel transfer fonksiyonuna sahip sistemin kontrolü için kesirli mertebeden oransal-entegral-türevsel (PID) kontrol edicinin tasarımı için çok amaçlıtasarım denklemleri türetilmiştir. Sonuçlar literatürde mevcut birçok tasarım metodunu birleştirmektedir. Özellikle genel kararlılık sınırlarının çiziminde kullanılmakta, istenilen kazanç ve faz aralıklarının kazanç-kesim frekansında yatay bir faz karakteritiği ile birlikte tasarımını sağlamaktadır. Dolayısıyla dayanıklılık da garanti edilmektedir. Ayrıca, tatminkar çıkış bozulması karakteristiği ve yüksek frekans gürültü engellenmesi gerçekleştirilemesine imkan sağlamaktadır. Literatürde mevcut metodlarla ilişkileri göstermek için bir örnek ele alınmıştır, ki böylece elde edilen tasarım denklemlerinin faydası gösterilmiştir.

Anahtar Kelimeler: Kontrol dizayn, PID kontrol, Kararlılık

[*]Sorumlu yazar (Corresponding author): Mehmet Emir KOKSAL, *mekoksal@omu.edu.tr*

1. INTRODUCTION

Proportional–Integral–Derivative (PID) controllers are very commonly and successfully used in controlling many industrial plants suffered from load disturbance and high frequency noise interference. They are also efficient to realize robustly the required performance specifications in cases of nonlinearities and uncertainties in the plant components [1-3]. In parallel with the invention of the high-speed computers and numerical techniques, fractional order calculus and the fractional order controllers have gained importance in recent decades [4-7]. In particular, fractional order PID (FOPID) controllers, which are the generalization of the 3-parameter conventional PID controllers, are now widely used to meet the given design specifications including mainly the desired gain and phase margins [8]. With introducing the fractional integral order λ and the fractional derivative order μ in PID controllers, the obtained FOPID (or $PI^{\lambda}D^{\mu}$) controllers with 5-parameters will have more powerful and effective control on the integer order and fractional order plants with or without a constant delay.

Although some other integer order controllers (lead-lag compensator [9], CRONE [10], optimized-order [11], and many other controllers have been generalized to fractional orders, these are excluded in the content of this contribution.

Fractional order systems (FOSs) could model various real materials more adequately than integer order ones and thus provide an excellent modelling tool in describing many actual dynamical processes. It is intuitively true, as also argued in [3], that these fractional order models require the corresponding fractional order controllers to achieve excellent performance.

The most common technique to realize the FOPID controller is to replace, according to the Oustaloup and Matsuda methods [7,12], the fractional-order transfer function by an integer-order transfer function whose characteristics are close enough to the desired. This process is performed for fractional order plants but not for the controllers in this presentation.

The special forms of $PI^{\lambda}D^{\mu}$ controllers such as PI^{λ} [8,9,13-15], PD^{μ} [16,17] controllers are used most of the time due to their design simplicities, though there are some derived alternatives $(PI)^{\lambda}$ [18], $(PD)^{\mu}$ [18], $PI^{\lambda}+P$ [19], and fractional lead-lag compensator (FLLC, [20]).

Although there are some genetic and evolutionary optimization algorithms [21], heuristic algorithms such as particle swarm [22, 23] and group hunting [24], designing fractional-order PID controllers in time domain [25-30] still has difficulties. Therefore, most studies are in the frequency domain using gain crossover frequency (ω_{gc}), gain margin (GM), phase crossover frequency (ω_{pc}), phase margin (PM) of the open-loop system [31].

Excluding many time domain specifications treated in the literature, a unified controller parameter expressions are derived in this paper for the standard $PI^{\lambda}D^{\mu}$ controller structure to meet. Wang et al.'s frequency domain specifications (GM, PM, phase flatness PF) [32] in the stability region found by stability boundaries method [8, 15,33,34]. The results reduce to already existing ones present in the literature for some bench-mark examples.

The content follows in Section 2 by introducing the general FOPID control structure and the design requirements. The derivation of universal design equations and design method is presented in Section 3. An illustrative example and its simulation results are treated in Section 4. Finally, Section 5 includes conclusions.

2. $PI^{\lambda}D^{\mu}$ CONTROL STRUCTURE AND DESIGN SPECIFICATIONS

Denoting the plant and controller transfer functions by G_p and G_c, respectively, the block diagram of the control system is shown in Figure 1 where G_v is the transfer function of the virtual compensator (it is also called gain-phase margin tester, GPMT

[8,33]) inserted to achieve the desired GM=20logA and PM=ϕ; r, e, u, y represent reference, error, actuating, and output (controlled) signals, respectively. The additive output disturbance d at the beginning of the feedback path and the additive noise n at the input of the plant are not shown in the figure.

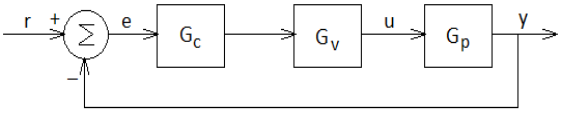

Figure 1. Block diagram of $PI^{\lambda}D^{\mu}$ control system structure

The transfer functions G_c, G_v, G_p are expressed as (Equation 1a, 1b and 1c)

$$G_c=K_p+\frac{K_i}{s^{\lambda}}+K_d s^{\mu}, \quad (1a)$$

$$G_v=Ae^{-j\phi}, \quad (1b)$$

$$G_p=\frac{N_2(s^2)+sN_1(s^2)}{D_2(s^2)+sD_1(s^2)}e^{-s\theta} \quad (1c)$$

G_c is obviously a $PI^{\lambda}D^{\mu}$ controller transfer function with proportional, integral, and derivative control coefficients K_p, K_p, K_p, and $0, \lambda, \mu$ orders, respectively. In G_v,A represents the GM, and ϕ represents the PM specifications. G_p is assumed to be a rational function with numerator polynomial $N=N_2(s^2)+sN_1(s^2)$ where N_2 (sN_1) represents its even (odd) part. $D=D_2(s^2)+sD_1(s^2)$ is defined similarly for the denominator polynomial. Finally, θ is the constant delay term in the plant transfer function.

It is straightforward to show that the control system output is expressed by (Equation 2) where the transfer functions on the right side of the equality sign are due to reference input (G), output disturbance (S) and noise interference (T), respectively.

$$Y(s)=\frac{G_cG_vG_p}{1+G_cG_vG_p}R(s)+\frac{1}{1+G_cG_vG_p}D(s)$$

$$+\frac{G_p}{1+G_cG_vG_p}N(s)$$

$$=G(s)R+S(s)D+T(s)N. \quad (2)$$

The aim of the $PI^{\lambda}D^{\mu}$ controller is to meet the following frequency domain specifications: GM [35], the Wang et al.[36]'s frequency domain specifications (PM, phase flatness PF) [18,36].

i) Phase cross over frequency ω_{pc} and Gain margin (GM) A: (Equation 3a-3e)

$$\text{Arg}(G_cG_vG_p)|_{s=j\omega_{pc}}=-\pi, \ |G_cG_vG_p|_{s=j\omega_{pc}}=A \quad (3a)$$

ii) Gain cross over frequency ω_{gc} and Phase margin (PM) ϕ:

$$|G_cG_vG_p|_{s=j\omega_{gc}}=1, \ \text{Arg}(G_cG_vG_p)|_{s=j\omega_{gc}}=\phi-\pi \quad (3b)$$

iii) Phase flatness (PF, iso-damping) ψ:

$$\frac{d\text{Arg}(G_cG_vG_p)_{s=j\omega}}{d\omega}|_{\omega=\omega_{gc}}=-\psi \quad (3c)$$

iv) A good output disturbance rejection (ODR) B:

$$\left|S(j\omega)=\frac{1}{1+G_cG_vG_p}\right|\leq B \text{ for all } \omega\leq\omega_s, \ |S(j\omega_s)|=B \quad (3d)$$

v) High frequency noise rejection (HFNR) C:

$$\left|T(j\omega)=\frac{G_p}{1+G_cG_vG_p}\right|\leq C \quad \text{for all } \omega\geq\omega_t, \ |T(j\omega)|=C \quad (3e)$$

Condition i) and ii), that is, GM and PM have always served as important measures of robustness [35,37]. It is known that the phase margin is related to the damping of the system and therefore can also serve as a performance measure.

Condition iii) is related with the robustness to variations in the gain of the plant (see [38]); this condition forces the phase of the open-loop system to be flat (completely flat for ψ=0) at ω_{gc} and

hence to be almost constant within an interval around ω_{gc}. It means that the system is more robust to gain changes and the overshoot of the response is almost constant within a gain range (iso-damping property of the time response). In testing the 3rd, 4th, 5th conditions, the virtual gain of GPMT, that is G_v, should be taken to be identity since it is virtually inserted to satisfy the specified GM and PM requirements. The phase plot is horizontal at ω_{gc} for ψ=0, it gets away from -180° line by moving upward as ω increases so for ψ<0 so the system is relatively more stable and robust, the approach to -180° becomes faster as ω increases for $\psi \ll 0$ so the system gets less robust.

3. DESIGN EQUATIONS AND DESIGN METHOD

The characteristic equation of the closed loop system obviously is $1+G_cG_vG_p=0$, or (Equation 4a and 4b)

$$1+\frac{K_ps^{\lambda}+K_i+K_ds^{\lambda+\mu}}{s^{\lambda}} *Ae^{-j\phi}\frac{N_2(s^2)+sN_1(s^2)}{D_2(s^2)+sD_1(s^2)}e^{-s\theta}=0 \quad (4a)$$

Then, the characteristic polynomial becomes

$$s^{\lambda}[D_2(s^2)+sD_1(s^2)]+\left(K_ps^{\lambda}+K_i+K_ds^{\lambda+\mu}\right) *[N_2(s^2)+sN_1(s^2)]Ae^{-s\theta-j\phi}=0 \quad (4b)$$

Since the designed system should be stable for A=1, θ=0, the roots of the characteristic equation must be in the stable region in the three-dimensional K_p-K_i-K_d space. The borders of this region are defined by the stability boundaries. The stability boundaries are computed as in [8,15,33, 34] where stability regions are computed on two-dimensional K_p-K_i or K_i-K_d Cartesian plane; the stability boundaries are some curves or lines in this case. On the other hand, the stability boundaries in our three-dimensional case are surfaces separating the stable and unstable volumetric regions. For $A\geq 1, \theta\geq 0$, the boundaries separate the feasible stable regions with the desired GM=20logA dB and PM=θ°.

The real, infinite, and imaginary (complex) root boundaries (RRB, IRB, CRB) are found by substituting $s=0,\infty,j\omega,$ in Equation 5a-5c; for λ,μ>0,degD> μ+degN, the results are

RRB: $K_i=0$ (5a)

IRB: It does not exist (5b)

$$\omega^{\lambda}\left(\cos\frac{\pi}{2}\lambda+j\sin\frac{\pi}{2}\lambda\right)[D_2(-\omega^2)+j\omega D_1(-\omega^2)] *\left\{K_p\omega^{\lambda}\left(\cos\frac{\pi}{2}\lambda+j\cos\frac{\pi}{2}\lambda\right) +K_i+K_d\omega^{\mu}\left(\cos\frac{\pi}{2}\mu+j\sin\frac{\pi}{2}\mu\right)\right\} *[N_2(-\omega^2)+j\omega N_1(-\omega^2)] *A\left[\cos(\omega\theta+\phi)-j\sin(\omega\theta+\phi)\right]=0, \quad (5c)$$

where deg stands for the degree.

Equating the real and imaginary parts of Equation 5c to zero and arranging the terms, we obtain CRB:

$$\begin{bmatrix}C_{11} & C_{12} & C_{13}\\ C_{21} & C_{22} & C_{23}\end{bmatrix}\begin{bmatrix}K_p\\ K_i\\ K_d\end{bmatrix}= \begin{bmatrix}-\omega^{\lambda}D_2(-\omega^2)\cos\frac{\pi}{2}\lambda+\omega^{\lambda+1}D_1(-\omega^2)\sin\frac{\pi}{2}\lambda\\ -\omega^{\lambda}D_2(-\omega^2)\sin\frac{\pi}{2}\lambda-\omega^{\lambda+1}D_1(-\omega^2)\cos\frac{\pi}{2}\lambda\end{bmatrix} \quad (6)$$

where

$$C_{11}=\omega^{\lambda}A\left[N_2\cos\left(\frac{\pi}{2}\lambda-\omega\theta-\phi\right)-\omega N_1\sin\left(\frac{\pi}{2}\lambda-\omega\theta-\phi\right)\right],$$

$$C_{21}=\omega^{\lambda}A\left[N_2\sin\left(\frac{\pi}{2}\lambda-\omega\theta-\phi\right)+\omega N_1\cos\left(\frac{\pi}{2}\lambda-\omega\theta-\phi\right)\right],$$

$$C_{12}=A[N_2\cos(\omega\theta+\phi)+\omega N_1\sin(\omega\theta+\phi)],$$

$$C_{22}=A[-N_2\sin(\omega\theta+\phi)+\omega N_1\cos(\omega\theta+\phi)],$$

$$C_{13}=\omega^{\lambda+\mu}A\begin{bmatrix}N_2\cos\left\{\frac{\pi}{2}(\lambda+\mu)-\omega\theta-\phi\right\}-\omega N_1\\ \sin\left\{\frac{\pi}{2}(\lambda+\mu)-\omega\theta-\phi\right\}\end{bmatrix},$$

$$C_{23}=\omega^{\lambda+\mu}A\begin{bmatrix}N_2\sin\left\{\frac{\pi}{2}(\lambda+\mu)-\omega\theta-\phi\right\}+\omega N_1\\ \cos\left\{\frac{\pi}{2}(\lambda+\mu)-\omega\theta-\phi\right\}\end{bmatrix}.$$

For a fixed set of design parameters λ, μ and design specifications A, ϕ, Equation 6 describes the parametric representation of the boundary for the stable permissible region (feasible volume, FV) of the design parameters K_p, K_i, K_d. And the specified PF, ODR, HFNR limitations can be chosen properly in this region.

For the desired phase flatness, gain cross over frequency ω_{gc} is computed first by using Equation 3b; the result is the solution of Equation 7a for ω.

$$\omega^{2\lambda}K_p^2+K_i^2+\omega^{2\lambda+2\mu}K_d^2+2\omega^{\lambda}K_pK_i\cos\frac{\pi}{2}\lambda +2\omega^{2\lambda+\mu}K_pK_d\cos\frac{\pi}{2}\mu+2\omega^{\lambda+\mu}K_iK_d\cos\frac{\pi}{2}(\lambda+\mu) =\frac{\omega^{2\lambda}(D_2^2+\omega^2D_1^2)}{A^2(N_2^2+\omega^2N_1^2)}, \quad (7a)$$

With the value of $\omega = \omega_{gc}$ found by this equation, Equation 3c yields

$$\lambda\omega^{\lambda-1}K_pK_i\sin\frac{\pi}{2}\lambda+\mu\omega^{2\lambda+\mu-1}K_pK_d\sin\frac{\pi}{2}\mu+ +(\lambda+\mu)\omega^{\lambda+\mu-1}K_iK_d\sin\frac{\pi}{2}(\lambda+\mu) =\frac{\omega^{2\lambda}(D_2^2+\omega^2D_1^2)}{QA^2(N_2^2+\omega^2N_1^2)} \quad (7b)$$

where all ω values are taken as ω_{gc} in this equation and in the following defining Q: (Equation 7c).

$$\frac{1}{Q}=\theta-\psi+\frac{D_1D_2+2\omega^2(D_1\dot{D}_2-\dot{D}_1D_2)}{D_2^2+\omega^2D_1^2} -\frac{N_1N_2+2\omega^2(N_1\dot{N}_2-\dot{N}_1N_2)}{N_2^2+\omega^2N_1^2}.$$

Note that $\dot{N}_1=dN_1(x)/dx|_{x=-\omega^2}$, and similar formulas are valid for the remaining dotted variables. Equation 7b defines a surface in K_p-K_i-K_d coordinate system for a given set of values GM (A), PM (ϕ), PF (ψ) and with the value of $\omega = \omega_{gc}$ found from Equation 7a. So, K_p, K_i, K_d must be chosen on the part remaining in the feasible region defined by Equation 6 of this surface.

Output disturbance rejection specification in Equation 3d yields

$$\frac{\omega^{\lambda}\sqrt{D_2^2+\omega^2D_1^2}}{f}\le B, \quad (8a)$$

where

$$f^2(K_p,K_i,K_d,\omega)=A^2(N_2^2+\omega^2N_1^2) *\left[\left(\omega^{2\lambda}K_p^2+K_i^2+\omega^{2\lambda+2\mu}K_d^2\right)+2\omega^{\lambda}K_pK_i\cos\frac{\pi}{2}\lambda+ 2\omega^{2\lambda+\mu}K_pK_d\cos\frac{\pi}{2}\mu+2\omega^{\lambda+\mu}K_iK_d\cos\frac{\pi}{2}(\lambda+\mu)\right] +A(N_2D_2+\omega^2N_1D_1) *\left[2\omega^{2\lambda}K_p\cos(\omega\theta+\phi)+2\omega^{\lambda}K_i\cos\left(\frac{\pi}{2}\lambda+\omega\theta+\phi\right) +2\omega^{2\lambda+\mu}K_d\cos\left(\frac{\pi}{2}\mu-\omega\theta-\phi\right)\right] +\omega^{2\lambda}(D_2^2+\omega^2D_1^2) \quad (8b)$$

for all values of $\omega \le \omega_s$ where the value of ω_s is found from Equation 8a by using equality sign instead of the inequality sign appearing in this equation. For $\omega = \omega_s$ Equation 8b with the equality sign defines a surface which defines the boundary of the feasible volume for satisfying the required disturbance rejection specification (remember to replace A by 1 and ϕ by 0).

In a similar manner as the derivation of Equation 8b, high frequency noise rejection (HFNR) in Equation 3e yields

$$\frac{\omega^{\lambda}\sqrt{N_2^2+\omega^2N_1^2}}{f}\le C \quad (9)$$

for all values of $\omega \ge \omega_t$, where the value of ω_t is found from Equation 9 by using equality sign instead of the inequality sign appearing in this equation. For $\omega = \omega_t$. Equation 9 with the equality sign defines a surface which defines the boundary of the feasible volume for satisfying the required HFNR specification.

Note that when using Equations 7-9 A must be chosen to be 1 since it is a virtual gain.

4. EXAMPLE

Although all-purpose design formulas are derived for designing a general $PI^{\lambda}D^{\mu}$ controller, a PI^{λ} controller is designed to show the use of these formulas.

The FOMCON Toolbox developed by A. Tepljakov, et al. is managed for the simulations of this example [39,40].

The example is similar to one in [8]. $G_c=K_p+K_i/s^{\lambda}$ so that $K_d=0$, $\mu=0$; $G_p=Ke^{-s\theta}/(Ts^2+s)$, hence, $N_2=K$, $N_1=0$, $D_2=Ts^2$, $D_1=1$. Design requirements are given as GM=6.02 dB, PM=30º, PF=-0.1 s, ODR=-6.06 dB, HFNR=13.98 dB which correspond to $A=2$, $\phi=\pi/3$, $\psi=-0.1$, $B=0.5$, $C=5$.

The feasible stability region is plotted in Figure 2. The phase flatness requirement is shown by the dotted graph. Choosing a point on this curve and approximately in the middle of the feasible region sets $K_p\cong0.03$, $K_i\cong0.03$.

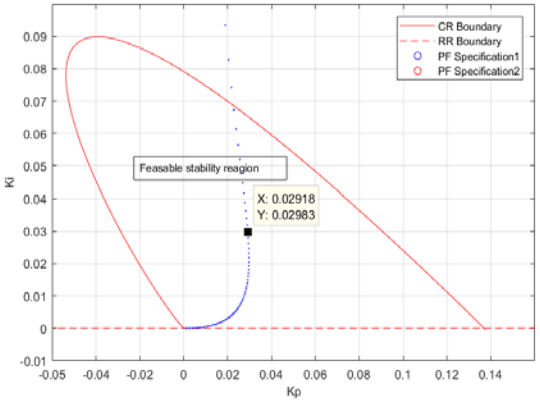

Figure 2. The stability region for the given example

The Bode plot with these values is shown in Figure 3 where the GM and PM appear to satisfy the design requirements: GM is increased from 1.1349 dB to GM=17.2545 dB>6.02 dB and, PM is increased from 6.7837^o to $PM=77.2545^o>30^o$. Therefore, the controlled system's relative stability is much better than that of the system itself.

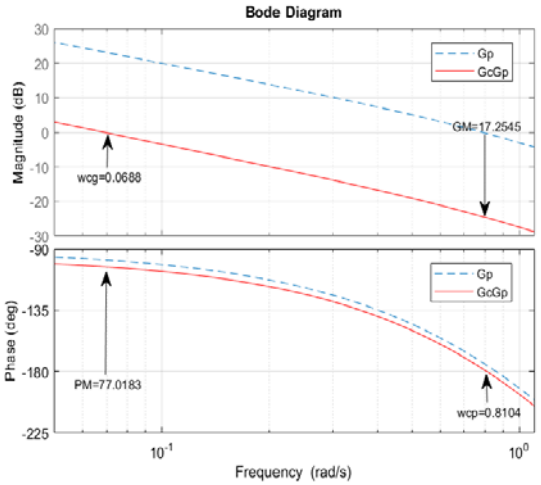

Figure 3. Bode plot of the open loop system

Time domain characteristics of the controlled system and the original plant are shown in Figure 4 as the step response. It is seen that the designed FOPI controller makes the unstable system (its step response is shown as Gp*0.3 in the figure) stable by a rise time (FOPI+Gp) quite smaller then P controlled response ((P+Gp).

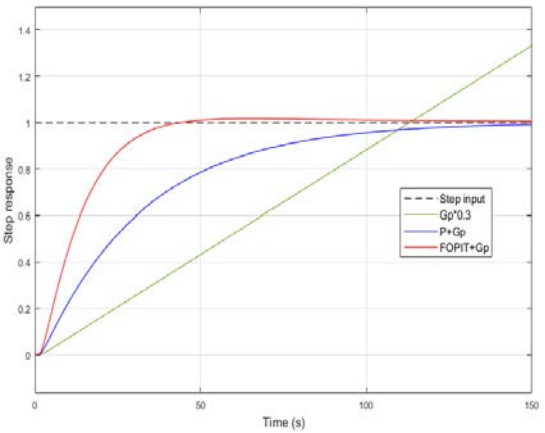

Figure 4. Step response characteristics

Output disturbance and noise rejections are also plotted in Figure 5. It is seen that the results are satisfactory when compared with the given design

specifications. In fact, Output disturbance rejection is smaller than B=0.5 for all $\omega \leq \omega_s$=0.06, and the noise rejection is smaller than C=5 for all $\omega > \omega_t$=0.131.

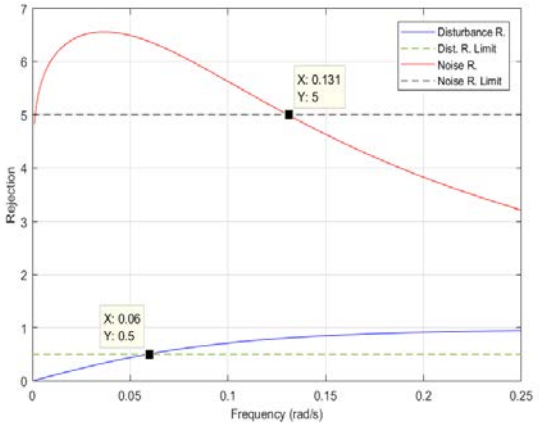

Figure 5. Output disturbance rejection and noise rejection

5. CONCLUSIONS

Some universal formulas are derived and interpreted for designing FOPID controllers for SISO integer order plants with a time delay. Three-dimensional stability boundary method is defined for designing a general $PI^{\lambda}D^{\mu}$ controller. The subspace of K_p-K_i-K_d=R^3 guaranteeing stability of the closed loop system together with the specified GM and PM is called the feasible region or volume; and the other requirements such as PF is defined as a 3- dimensional surface. So, the choice of design parameters on this surface remaining on its part remaining in the feasible volume gives a satisfactory design. The success depends also one's skills of drawing 3-D graphics by using MATLAB. Some more 3-D bench-mark problems should be worked on to prove the efficiency of the proposed method as the future work.

6. REFERENCES

1. Astrom, K. J., Hagglund, T., 1995. PID Controllers: Theory, Design, and Tuning.

2. Ang, K. H., Chong, G., Li, Y., 2013. PID Control System Analysis, Design, and Technology, IEEE Trans. Control Syst. Technol. 13, 559–576.

3. Yamamoto, T., Takao, K., Yamada, T., 2009. *Design* of a Data-driven PID Controller, IEEE Trans. Control Syst. Technol. 17, 29-39.

4. Erenturk, K., 2013. Fractional-order $PI^{\lambda}D^{\mu}$and Active Disturbance Rejection Control of Nonlinear Two-mass Drive System, IEEE Trans. Ind. Electron. 60, 3806-3813.

5. Yeroglu, C., Tan, N., 2011. Note on Fractional-order Proportional-Integral-Differential Controller Design, IET Control Theory Appl., 5, 1978-1989.

6. Monje, C.A., Vinagreb, B.M., Feliuc, V., Chen, Y.Q., 2008. Tuning and Auto-tuning of Fractional Order Controllers for Industry Applications, Control Eng. Pract., 16, 798-812.

7. Chunna, Z., Xue, D., Chen, Y. Q., 2005. A Fractional Order PID Tuning Algorithm for a Class of Fractional Order Plants, IEEE Proc. of the Intern. Conf. Mechatronics & Automation, 216-221.

8. Cokmez, E., Atic, S., Peker, F., Kaya, I., 2018. Fractional-order PI Controller Design for Integrating Processes Based on Gain and Phase Margin Specifications, IFAC PapersOnLine, 51, 751-756.

9. Pullaguram, D., Mishra, S., Senroy, N., Mukherjee, M., 2018. Design and Tuning of Robust Fractional Order Controller for Autonomous Microgrid Vsc System, IEEE Transactions on Industry Applications, 54, 91-101.

10. Oustaloup, A., Cois, O., Lanusse, P., Melchior, P., Moreau, X., Sabatier, J., 2006. The Crone Aproach: Theoretical Developments and Major Applications, IFAC Proc., 39, 324-354.

11. Vinagre, B.M., Feliu, V., 2007. Optimal Fractional Controllers for Rational Order Systems, IEEE Trans. Autom. Control 52, 2385-2389.

12. Krishna, B.T., 2011. Studies on Fractional Order Differentiators and Integrators: a Survey, Signal Processing, 91, 386-426.

13. John, D.A., Biswas, K., 2018. Analysis of Disturbance Rejection by PI^{λ} Controller Using Solid State Fractional Capacitor, IEEE Proc. of

the International Symposiums of Circuits and Systems, 1-5.

14. Khurram, A., Rehman, H., Mukhopadhyay, S., 2018. Comparative Analysis of Integer-order and Fractional-order Proportional Integral Speed Controllers for Induction Motor Drive Systems, Journal of Power Electronics, 18, 723-735.

15. Dogruer, T., Tan, N., 2018. Design of PI Controller Using Optimization Method in Fractional Order Control Systems, IFAC PapersOnLine, 51, 841-846.

16. Raynaud, H.F., Zergainoh, A., 2000. State-space Representation for Fractional Order Controllers, Automatica, 36, 1017-1021.

17. Zagorowska, M., 2018. Analysis of Performance Indicators for Optimization of Noninteger-order Controllers, Journal of Circuits, Systems and Computers, 27.

18. Sathishkumar, P., 2018. Fractional Controller Tuning Expressions for a Universal Plant Structure, IEEE Control Systems Letters, 2, 345-350.

19. Ranjbaran, K., Tabatabaei, M., 2018. Tuning PI and Fractional Order PI Controllers With an Additional Fractional Order Pole, Chemical Engineering Communications, 205, 207-225.

20. Xue, D., Chen, Y.Q., 2002. A Comparative Introduction of four Fractional Order Controllers, Proc. of the 4th World Congress on Intelligent Control and Automation, 3228-3235.

21. Kumar, L., Narang, D., 2018. Tuning of Fractional Order $PI^{\lambda}D^{\mu}$ Controllers Using Evolutionary Optimization for Pid Tuned Synchronous Generator Excitation System, IFAC-PapersOnLine, 51, 859-864.

22. Dabiri, A., Moghaddam, B.P., Machado, J.A.T., 2018. Optimal Variable-order Fractional PID Controllers for Dynamical Systems, Journal of Comp. Appl. Math 339, 40-48.

23. Cao, J., Cao, B., 2006. Design of Fractional Order Controller Based on Particle Swarm Optimization, IEEE Conference on Industrial Electronics and Applications, 1-6.

24. Ranjan, J., Nayak, B.S., 2018. Application of Group Hunting Search Optimized Cascade Pd-fractional Order PID Controller in Interconnected Thermal Power System, Trends in Renewable Energy, 4, 22-33.

25. Lu, K., Zhou, W., Zeng, G., Du, W., 2018. Design of PID Controller Based on a Self-adaptive State-space Predictive Functional Control Using Extremal Optimization Method, Journal of the Franklin Institute, 355, 2197-2220.

26. Shukla, M. K., Sharma, B. B., 2018. Control and Synchronization of a Class of Uncertain Fractional Order Chaotic Systems Via Adaptive Backstepping Control, Asian Journal of Control, 20, 707-720.

27. Ibraheem, L.K., Abdul-Adheem, W.R., 2016. On the Improved Nonlinear Tracking Differentiator Based Nonlinear Pid Controller Design, International Journal of Advanced Computer Science and Applications, 7, 234-241.

28. Li, L., 2018. Lebesgue-P NORM Convergence of Fractional-Order PID-Type Iterative Learning Control for Linear Systems, Asian Journal of Control, 20, 483-494.

29. Moradi, L., Mohammadi, F., Baleanu, D., 2018. A Hybrid Functions Numerical Scheme for Fractional Optimal Control Problems: Application to Nonanalytic Dynamic Systems, Journal of Vibration and Control, 22, 1-15.

30. Sharma, K.D., Sarkar, G., 2018. Stable Adaptive NSOF Domain FOPID Controller for a Class of Non-linear Systems, IET Control Theory & Applications.

31. De Keyser, R., Muresan, C.I., Ionescu, C.M., 2015. A Novel Auto-tuning Method for Fractional Order PI/PD Controllers, ISA Transactions, 62, 268-275.

32. Golnaraghi, F., Kuo, B.C., 2010. Automatic Control Systems, Wiley John Wiley & Sons, Inc.

33. Hamamci, S.E., 2007. An Algorithm for Stabilization of Fractional-Order Time Delay Systems Using Fractional-Order PID Controllers, IEEE Transactions on Automatic Control, 52, 1964-1969.

34. Tan, N., Kaya, I., Yeroglu, C., Atherton, D.P., 2006. Computation of Stabilizing PI and PID Controllers Using the Stability Boundary Locus, Energy Conversion and Management, 47, 3045-3058.

35. Monje, A., Blas, M., Vinagre, V., Chen, Y.Q., 2008. Tuning and Auto-tuning of Fractional

Order Controllers for Industry Applications, Control Engineering Practice, 16, 798-812.

36. Wang, C.Y., Luo, Y., Chen, Y.Q., 2009. Tuning Fractional Order Proportional Integral Controllers for Fractional Order Systems, Chinese Control and Decision Conference, 329-334.

37. Franklin, G., Powell, J., Naeini, A., 2006. Feedback Control Of Dynamic Systems, Addison-Wesley.

38. Chen, Y.Q., Moore, K.L., 2005. Relay Feedback Tuning of Robust PID Controllers With Iso-damping Property, IEEE Transactions on Systems, Man, and Cybernetics, 35, 23–31.

39. Tepljakov, A., Petlenkov, E., Belikov, J., 2014. Closed-loop Identification of Fractional-order Models Using FOMCON Toolbox for MATLAB, Proc. of the 14th Biennial Baltic Electronics Conference, 213-216.

40. Tepljakov, A., 2012. FONCON: Fractional-order Modeling and Control.